

Cartan's Supersymmetry and the Decay of a $H^0(0^+)$

Sadataka Furui

*Graduate School of Teikyo University
2-17-12 Toyosatodai, Utsunomiya, 320-0003 Japan*

E-mail: furui@umb.teikyo-u.ac.jp

ABSTRACT: We compare the decay of a Higgs boson $H^0(0^+) \rightarrow \gamma\gamma$, $H^0(0^+) \rightarrow W\bar{W} \rightarrow \ell\bar{\nu}\ell\nu$, and $H^0(0^+) \rightarrow Z\bar{Z} \rightarrow \ell\bar{\ell}\ell\bar{\ell}$ using Cartan's supersymmetry, that defines coupling of a vector particle X and Dirac spinors ψ and ϕ .

Experimentally the ratio of the signal strength, i.e. branching ratio normalized to the standard model value $\sigma(H^0 \rightarrow xx) = B(H^0 \rightarrow xx)_{exp}/B(H^0 \rightarrow xx)_{SM}$, of $W\bar{W}$ channel and $\gamma\gamma$ channel $\frac{\sigma(H^0 \rightarrow W\bar{W})}{\sigma(H^0 \rightarrow \gamma\gamma)}$ is $\frac{0.87 \pm 0.2}{1.58 \pm 0.3}$, agrees with the ratio of the number of independent diagrams $\frac{9}{16}$ derived from Cartan's supersymmetric theory of spinors.

The enhancement of the $\sigma(H^0 \rightarrow Z\bar{Z}) = 1.11 \pm 0.3$ relative to $\sigma(H^0 \rightarrow W\bar{W}) = 0.87 \pm 0.2$ is expected to be due to $g\bar{g} \rightarrow \ell\bar{\ell}\ell\bar{\ell}$ in the final state of $Z\bar{Z}$ channel.

KEYWORDS: Supersymmetric Effective Theories, Higgs Physics, B physics

Contents

1	Introduction	1
2	Analysis using Cartan's supersymmetry	2
3	Discussion and conclusion	5

1 Introduction

In the book of the theory of spinors[1], Cartan proposed two types of Dirac spinors ϕ and ψ and their charge conjugates $\mathcal{C}\phi$ and $\mathcal{C}\psi$ and two types of vector particles \mathbf{E} and \mathbf{E}' .

In [2] we studied decays of $H^0(0^+)$ into photons, and in [3] we studied the decay of $\chi_b(nP)$ into $\Upsilon(mS)\gamma$ and possible decay of Higgs partner $h^0(0^+)$ into $\Upsilon(mS)\gamma$ ($m = 1, 2$).

In this paper, we study decays of $H^0(0^+)$ into $\ell\bar{\ell}\ell\bar{\ell}$ and compare with the decay of $H^0(0^+)$ to other decay modes.

The Higgs boson $H^0(0^+)$ decays into $W\bar{W}$, $Z\bar{Z}$ and $\gamma\gamma$ corresponding to the strength in the unit of the standard model 0.89 ± 0.2 , 1.11 ± 0.3 and 1.58 ± 0.3 , respectively[4, 5] The boson W decays in the average 10.86% to $\ell\bar{\nu}$, and Z decays in the average 3.6% to $\ell\bar{\ell}$ ($\ell = e, \mu$ or τ).

The decay branching ratio of $H^0(0^+) \rightarrow Z\bar{Z}$ is obtained from $H^0(0^+) \rightarrow \ell\bar{\ell}\ell\bar{\ell}$, and the strength parameter in this channel seems to be very sensitive to the mass of $H^0(0^+)$, and whether the final $\ell\bar{\ell}\ell\bar{\ell}$ originates from $Z\bar{Z}$ is not clear. By inclusion of $g\bar{g} \rightarrow \ell\bar{\ell}\ell\bar{\ell}$, the signal strength of $H^0(0^+) \rightarrow Z\bar{Z}$ calculated as the average of the true contribution M_Z and the contribution from other decays $M_{\ell\bar{\ell}\ell\bar{\ell}} - M_z$ was reduced to 0.99[6], and by inclusion of $g\bar{g} \rightarrow Z\bar{Z}$, the signal strength was reduced to 0.93 ± 0.3 [7].

The coupling of the Higgs boson to two leptons is given by[8]

$$-y_\ell^{ij} \mathcal{E}_i(\mathcal{L}_j \circ \mathcal{H}_d) = -y_\ell^{ij} H_d^0 \bar{\ell}_{L_i} \ell_{L_j}$$

where L_i, L_j specify left handed $SU(2)$ lepton degrees of freedom. Right chiral leptons are defined as \mathcal{E}_i ($i = 1, 2, 3$)

$$\begin{aligned} \mathcal{E}_1 &= \tilde{\phi}_{\bar{e}} + \theta \cdot \chi_{\bar{e}} + \frac{1}{2}\theta \cdot \theta F_{\bar{e}} \\ \mathcal{E}_2 &= \tilde{\phi}_{\bar{\mu}} + \theta \cdot \chi_{\bar{\mu}} + \frac{1}{2}\theta \cdot \theta F_{\bar{\mu}} \\ \mathcal{E}_3 &= \tilde{\phi}_{\bar{\tau}} + \theta \cdot \chi_{\bar{\tau}} + \frac{1}{2}\theta \cdot \theta F_{\bar{\tau}} \end{aligned}$$

Left chiral leptons are defined as

$$\mathcal{L}_1 = \begin{pmatrix} \tilde{\phi}_{\nu_e} \\ \tilde{\phi}_e \end{pmatrix} + \theta \cdot \begin{pmatrix} \chi_{\nu_e} \\ \chi_e \end{pmatrix} + \frac{1}{2}\theta \cdot \theta \begin{pmatrix} F_{\nu_e} \\ F_e \end{pmatrix}$$

and \mathcal{L}_2 and \mathcal{L}_3 are defined similarly.

2 Analysis using Cartan's supersymmetry

Following Cartan's supersymmetry, we express scalar particles by Ψ and Φ , and leptons by $\psi, \mathcal{C}\phi$ and antileptons by $\mathcal{C}\psi, \phi$. Assignment of Ψ and Φ can express the roles of Higgs bosons i.e. production of mass and chirality very powerfully.

The coupling of a vector field X to Dirac spinors,

$$\begin{aligned}\psi &= \xi_1 \mathbf{i} + \xi_2 \mathbf{j} + \xi_3 \mathbf{k} + \xi_4 \mathbf{I} = \begin{pmatrix} \xi_4 + i\xi_3 & i\xi_1 - \xi_2 \\ i\xi_1 + \xi_2 & \xi_4 - i\xi_3 \end{pmatrix} \\ \mathcal{C}\psi &= -\xi_{234} \mathbf{i} - \xi_{314} \mathbf{j} - \xi_{124} \mathbf{k} + \xi_{123} \mathbf{I} = \begin{pmatrix} \xi_{123} - i\xi_{124} & -i\xi_{234} + \xi_{314} \\ -i\xi_{234} - \xi_{314} & \xi_{123} + i\xi_{124} \end{pmatrix}\end{aligned}\quad (2.1)$$

and the spinor operator

$$\begin{aligned}\phi &= \xi_{14} \mathbf{i} + \xi_{24} \mathbf{j} + \xi_{34} \mathbf{k} + \xi_0 \mathbf{I} = \begin{pmatrix} \xi_0 + i\xi_{34} & i\xi_{14} - \xi_{24} \\ i\xi_{14} + \xi_{24} & \xi_0 - i\xi_{34} \end{pmatrix} \\ \mathcal{C}\phi &= -\xi_{23} \mathbf{i} - \xi_{31} \mathbf{j} - \xi_{12} \mathbf{k} + \xi_{1234} \mathbf{I} = \begin{pmatrix} \xi_{1234} - i\xi_{12} & -i\xi_{23} + \xi_{31} \\ -i\xi_{23} - \xi_{31} & \xi_{1234} + i\xi_{12} \end{pmatrix}\end{aligned}\quad (2.2)$$

are specified by[1, 10]

$$\begin{aligned}\mathcal{F}_H &= {}^t\phi \mathcal{C} X \psi = {}^t(\mathcal{C}\phi) \gamma_0 x^i \gamma_i \psi + {}^t\phi \gamma_0 x^{i'} \gamma_{i'} (\mathcal{C}\psi) \\ &= x^1 (\xi_{12} \xi_{314} - \xi_{31} \xi_{124} - \xi_{14} \xi_{123} + \xi_{1234} \xi_1) \\ &\quad + x^2 (\xi_{23} \xi_{124} - \xi_{12} \xi_{234} - \xi_{24} \xi_{123} + \xi_{1234} \xi_2) \\ &\quad + x^3 (\xi_{31} \xi_{234} - \xi_{23} \xi_{314} - \xi_{34} \xi_{123} + \xi_{1234} \xi_3) \\ &\quad + x^4 (-\xi_{14} \xi_{234} - \xi_{24} \xi_{314} - \xi_{34} \xi_{124} + \xi_{1234} \xi_4) \\ &\quad + x^{1'} (-\xi_0 \xi_{234} + \xi_{23} \xi_4 - \xi_{24} \xi_3 + \xi_{34} \xi_2) \\ &\quad + x^{2'} (-\xi_0 \xi_{314} + \xi_{31} \xi_4 - \xi_{34} \xi_1 + \xi_{14} \xi_3) \\ &\quad + x^{3'} (-\xi_0 \xi_{124} + \xi_{12} \xi_4 - \xi_{14} \xi_2 + \xi_{24} \xi_1) \\ &\quad + x^{4'} (\xi_0 \xi_{123} - \xi_{23} \xi_1 - \xi_{31} \xi_2 - \xi_{12} \xi_3)\end{aligned}\quad (2.3)$$

In the expression of $-y_d^{ij} H_d^0 \bar{\ell}_{L_i} \ell_{L_j}$ coupling,

$$\ell_{L_j} = \begin{pmatrix} \psi \\ \mathcal{C}\psi \end{pmatrix}_j \quad \text{and} \quad \bar{\ell}_{L_i} = (\mathcal{C}\phi, \phi)_i.$$

In the case of coupling of γ to Higgs bosons, we considered 16 diagrams two of which are shown in Fig.1 and 2.

The Higgs boson $H^0(0^+)$ has a partner $h^0(0^+)$, and in [3] we discussed possibility of its decay into $b\bar{b}\ell\bar{\ell}$. We compared the amplitude of production of $\Upsilon(m_S)\ell\bar{\ell}$ near the threshold, in which $\ell\bar{\ell}$ becomes a γ . In the case of $h^0(0^+)$ decay, in addition to the coupling y_e^{ij} , another coupling y_b^{ij} defined by[8]

$$-y_b^{ij} \mathcal{D}_i(\mathcal{Q}_j \circ \mathcal{H}_d) = -y_b^{ij} \nu_d \bar{b}_i b_j$$

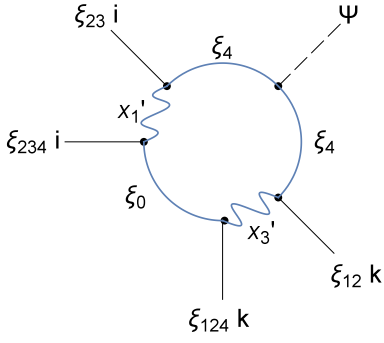


Figure 1. Scalar boson decay into four leptons. $\Psi(11) \rightarrow \mathcal{C}\phi\mathcal{C}\psi\mathcal{C}\phi\mathcal{C}\psi \rightarrow \gamma\gamma$ type.

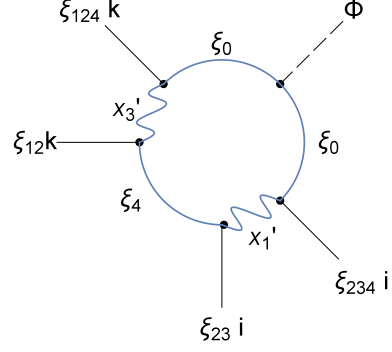


Figure 2. Scalar boson decay into four leptons. $\Phi(11) \rightarrow \mathcal{C}\psi\mathcal{C}\phi\mathcal{C}\psi\mathcal{C}\phi \rightarrow \gamma\gamma$ type.

appear. Here, ν_d is defined by the minimum of the potential $H_d = {}^t(\nu_d, 0)$, and after diagonalization $m_{d,s,b} = \nu_d y_{d,s,b}$.

Couplings of quarks u, c, t to Higgs bosons are defined by

$$y_u^{ij} \mathcal{U}_i(\mathcal{Q}_j \circ \mathcal{H}_u) = y_u^{ij} \nu_u \bar{u}_i u_j$$

and the coupling of quarks to electromagnetic field is defined as

$$\mathcal{F}_L = \bar{\psi}_L^k (\gamma_L (i\partial_\mu - eA_\mu) - m) \psi_L^k + \bar{\phi}_L^k (\gamma_L (i\partial_\mu - eA_\mu) - m) \phi_L^k$$

where

$$\psi_L^k = \begin{pmatrix} \psi \\ \mathcal{C}\psi \end{pmatrix}_k \quad \text{and} \quad \phi_L^k = \begin{pmatrix} \mathcal{C}\phi \\ \phi \end{pmatrix}_k.$$

In electromagnetic interactions ψ v.s. $\mathcal{C}\phi$ and ϕ v.s. $\mathcal{C}\psi$ have no differences, but we expect that our electronic detector is sensitive only to ψ_L^k .

In the weak interactions there are difference in ϕ_L^k and ψ_L^k , as the final states of supersymmetric transformation[2]. When the supersymmetric transformation is G_{13} , transformations $\mathbf{E} \rightarrow \mathcal{C}\psi$ and $\mathbf{E}' \rightarrow \psi$ in the lepton sector, and the spinor $\phi_L^k \rightarrow \tilde{\phi}_L^k$ appears in the quark sector, where $\tilde{\phi}_L^k$ means that particle-antiparticle transformation is done on ϕ_L^k . When the transformation is G_{132} , transformations $\mathbf{E} \rightarrow \phi$ and $\mathbf{E}' \rightarrow \mathcal{C}\phi$ occurs in the lepton sector and the spinor $\phi_L^k \rightarrow \tilde{\psi}_L^k$ appears in the quark sector.

When the supersymmetric transformation is G_{12} , transformations $\mathbf{E} \rightarrow \tilde{\phi}$ in the lepton sector and $\psi_L^k \rightarrow \tilde{\psi}_L^k$ appears in the quark sector. When the transformation is G_{123} , transformations of $\mathbf{E} \rightarrow \tilde{\mathcal{C}}\psi$ and $\mathbf{E}' \rightarrow \tilde{\psi}$ occurs in the lepton sector and $\psi_L^k \rightarrow \tilde{\phi}_L^k$ in the quark sector.

In the coupling of $H_d^0 \bar{\ell}\ell$, i, j in the coupling y_ℓ^{ij} specifies generations of left-handed $\bar{\ell}$ and ℓ , respectively, and in the coupling of $H_d \bar{b}b$, i, j in the coupling y_b^{ij} specifies generations of left-handed \bar{b} and b , respectively.

In the case of $H^0(0^+)$ decay, we define the effective y_ℓ^{ij} from final four lepton states which are symmetric on the upper semicircle and on the lower semicircle, when all the y_e^{ij} and y_μ^{ij} are taken into account in the present analysis. There 3 diagrams of $H(0^+, 11) \rightarrow$

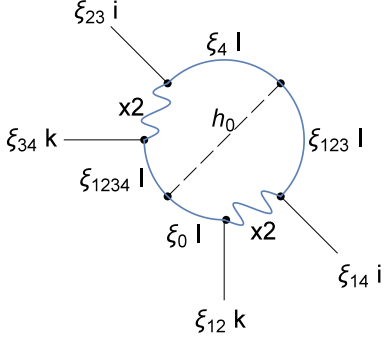


Figure 3. The $h(0^+, 11) \rightarrow \Upsilon(1S)\gamma(\mathbf{k})$ with a vector particle $\mathbf{x}2$ exchange.

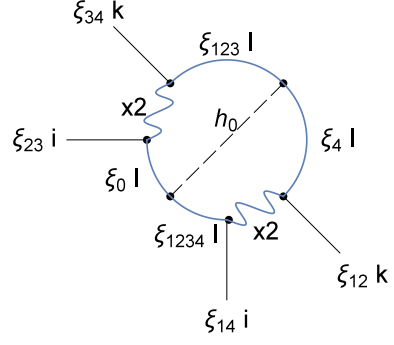


Figure 4. The $h(0^+, 11) \rightarrow \Upsilon(1S)\gamma(\mathbf{i})$ with a vector particle $\mathbf{x}2$ exchange.

$\gamma\gamma$, 2 diagrams of $H(0^+, \mathbf{i}\mathbf{i}) \rightarrow \gamma\gamma$, 2 diagrams of $H(0^+, \mathbf{j}\mathbf{j}) \rightarrow \gamma\gamma$, and 2 diagrams of $H(0^+, \mathbf{k}\mathbf{k}) \rightarrow \gamma\gamma$, in which ℓ and $\bar{\ell}$ have parallel momenta. i.e. altogether 9 diagrams that define the coupling of a Higgs boson to $\ell\bar{\ell}\ell\bar{\ell}$ with parallel momenta.

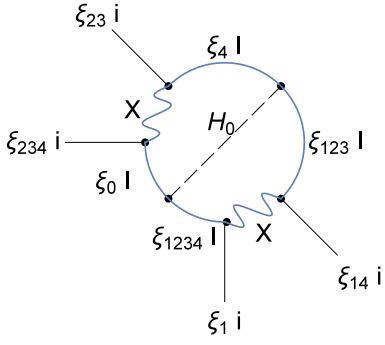


Figure 5. The $H(0^+, 11) \rightarrow \ell\bar{\ell}(\mathbf{i})\ell\bar{\ell}(-\mathbf{i})$ with a vector particle \mathbf{X} exchange.

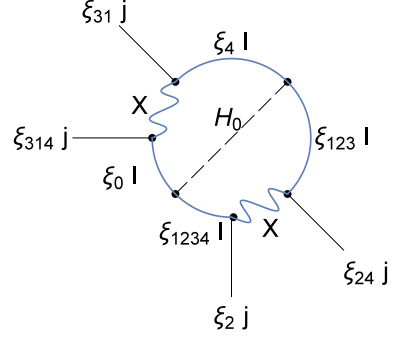


Figure 6. The $H(0^+, 11) \rightarrow \ell\bar{\ell}(\mathbf{j})\ell\bar{\ell}(-\mathbf{j})$ with a vector particle \mathbf{X} exchange.

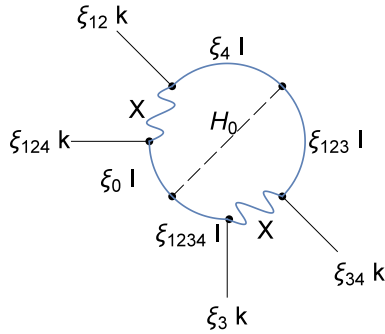


Figure 7. The $H(0^+, 11) \rightarrow \ell\bar{\ell}(\mathbf{k})\ell\bar{\ell}(-\mathbf{k})$ with a vector particle \mathbf{X} exchange.

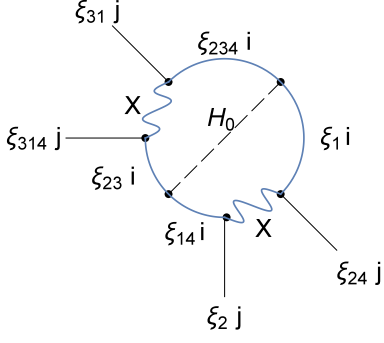


Figure 8. The $H(0^+, ii) \rightarrow \ell\bar{\ell}(j)\ell\bar{\ell}(-j)$ with a vector particle X exchange.

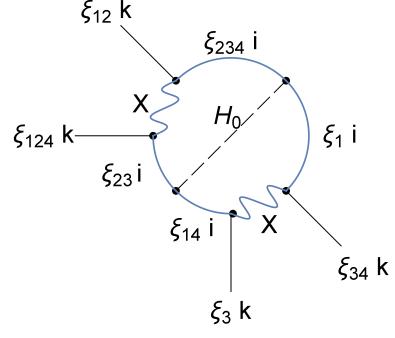


Figure 9. The $H(0^+, ii) \rightarrow \ell\bar{\ell}(k)\ell\bar{\ell}(-k)$ with a vector particle X exchange.

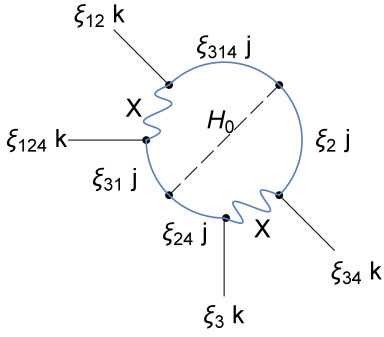


Figure 10. The $H(0^+, jj) \rightarrow \ell\bar{\ell}(k)\ell\bar{\ell}(-k)$ with a vector particle X exchange.

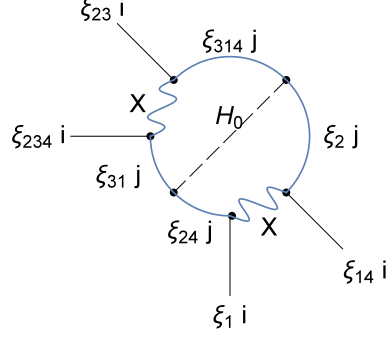


Figure 11. The $H(0^+, jj) \rightarrow \ell\bar{\ell}(i)\ell\bar{\ell}(-i)$ with a vector particle X exchange.

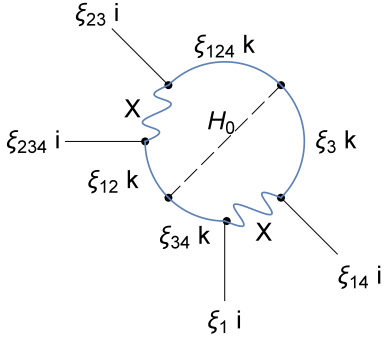


Figure 12. The $H(0^+, kk) \rightarrow \ell\bar{\ell}(i)\ell\bar{\ell}(-i)$ with a vector particle X exchange.

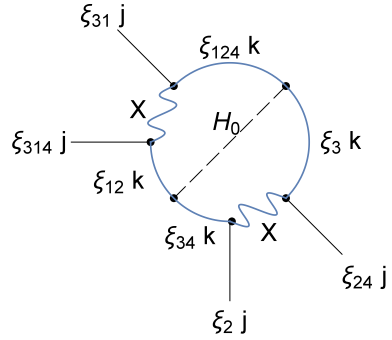


Figure 13. The $H(0^+, kk) \rightarrow \ell\bar{\ell}(j)\ell\bar{\ell}(-j)$ with a vector particle X exchange.

3 Discussion and conclusion

We studied the decay of Higgs boson $H^0(0^+)$ to $\gamma\gamma$ via $\ell\bar{\ell}$ and $\ell'\bar{\ell}'$ states, which have strong correlations, in contrast to $h^0(0^+)$ decay to $b\bar{b}\gamma$ via $b\bar{b}e\bar{e}$.

In the standard model, the vector boson Z and the vector field A are expressed as

$$\begin{aligned} Z_\mu &= \cos \theta_W \cdot W_\mu^0 + \sin \theta_W \cdot B_\mu \\ A_\mu &= -\sin \theta_W \cdot W_\mu^0 + \cos \theta_W \cdot B_\mu \end{aligned}$$

and $\sin^2 \theta_W \simeq 0.22$ is the Weinberg angle. Relative strength of B_μ near the energy of the mass of Higgs boson is not so clear.

If the Higgs boson $H^0(0^+)$ decay as $h^0(0^+)$ to $b\bar{b}e\bar{e}$, and finally to $\gamma\gamma$, we can consider the Higgs boson decay into $\gamma\gamma$ given by 4 types of diagrams

$$\begin{aligned} \Psi &\rightarrow \mathcal{C}\phi\mathcal{C}\psi, \mathcal{C}\phi\mathcal{C}\psi, & \Phi &\rightarrow \mathcal{C}\psi\mathcal{C}\phi, \mathcal{C}\psi\mathcal{C}\phi \\ \Psi &\rightarrow \phi\psi, \phi\psi, & \Phi &\rightarrow \psi\phi, \psi\phi \end{aligned}$$

each having 4 diagrams with different polarizations, i.e. altogether 16 independent diagrams.

As the decay modes of Higgs boson $H^0(0^+) \rightarrow \ell\bar{\ell}\ell\bar{\ell} \rightarrow \gamma\gamma$, we obtain 9 types of diagrams. In the energy region of Higgs boson mass, the decay to $\gamma\gamma$ occurs through $\ell\bar{\ell}\ell\bar{\ell}$ in the final state of $Z\bar{Z}$. The boson Z has a partner of a vector field A in this energy region. The field A is assigned as a photon, and the Z_μ and A_μ contribute to the production of $\ell\bar{\ell}\ell\bar{\ell}$ final state of $Z\bar{Z}$, but the contamination of $g\bar{g} \rightarrow \ell\bar{\ell}\ell\bar{\ell}$ in the final state of $Z\bar{Z}$ reduces the signal strength of $Z\bar{Z}$ final state 1.11 ± 0.3 observed in [5] to 0.93 ± 0.3 [7].

In contrast, the decay of $H^0(0^+)$ to $\ell\bar{\nu}\ell\nu$ via intermediate state of $W\bar{W}$ is well known[5, 9]. Using the same reasoning as $H^0(0^+)$ decay to $\ell\bar{\ell}\ell\bar{\ell}$, we expect there are 9 independent diagrams in $H(0^+) \rightarrow \ell\bar{\nu}\ell\nu$, which are detected as $H(0^+) \rightarrow W\bar{W}$. The signal strength of $W\bar{W}$ fstate 0.87 ± 0.2 is consistent with the new signal strength of $Z\bar{Z}$ state.

Experimentally the signal strength of $H^0 \rightarrow \gamma\gamma$ is $1.58_{-0.23}^{+0.27}$ and that of $H^0 \rightarrow W\bar{W}$ is $0.87_{-0.22}^{+0.24}$. The ratio $\frac{\sigma(H^0 \rightarrow W\bar{W})}{\sigma(H^0 \rightarrow \gamma\gamma)}$ is $\frac{0.87 \pm 0.2}{1.58 \pm 0.3}$, which agrees with the ratio of the number of independent diagrams $\frac{9}{16}$ roughly agrees with the ratio of the number of independent diagrams derived from Cartan's supersymmetric theory of spinors.

References

- [1] É. Cartan, *The theory of Spinors*, Dover Pub. (1966)
- [2] S. Furui, Triality selection rules of Octonion and Quantum Mechanics, [hep-ph/1409.3761].
- [3] S. Furui, Cartan's Supersymmetry and the Decay of a h^0 with the mass $m_{h^0} \simeq 11\text{GeV}$ to $\Upsilon(1S)\gamma$ and to $\Upsilon(2S)\gamma$, [hep-ph/1502.07011].
- [4] K.A. Olive et al, (Particle Data Group), Review of Particle Physics, Chinese Physics **C38**, (2014) 090001.
- [5] ATLAS Collaboration, Measurement of Higgs boson and couplings in diboson final states with the ATLAS detector at the LHC, Physics Letters **B 726** (2013) 88-119. [Erratum *ibid* **B 734** (2014) 406].

- [6] J.S. Gainer, J. Lykken, K.T. Matchev, S. Mrenna and M. Park, Beyond Geolocating: Constraining Higher Dimensional Operators in $H \rightarrow 4\ell$ with Off-Shell Production and More, *Phys. Rev. D* **91** (2014) 035011.
- [7] L. Finco, L., Recent Results of the Higgs Boson Properties in the $H \rightarrow ZZ \rightarrow 4\ell$ decay channel at CMS, in *Proceedings of the Second Annual Conference on Large Hadron Collider Physics*, Columbia University, New York, U.S.A. June 2014, [hep-ex/1409.2646v2].
- [8] P. Labelle, *Supersymmetry Demystified*, McGraw Hill (2010).
- [9] The CMS Collaboration, Evidence for the direct decay of the 125 GeV Higgs boson to fermions, *nature Physics*, DOI:10.1038/NPHYS3005 (2014).
- [10] S. Furui, Fermion Flavors in Quaternion Basis and Infrared QCD, *Few Body Syst.* **52**, (2012) 171-187, [hep-ph/1104.1225].
- [11] S. Furui, The flavor symmetry in the standard model and the triality symmetry, *Int. J. Mod. Phys. A* **27** (2012) 1250158, [hep-ph/1203.5213].